

NANOSTRUCTURES

PACS numbers: 81.05.Je; 81.40.Tv; 42.70.Mp
DOI: 10.1070/QE2009v039n10ABEH014008

Optical absorption in CaF_2 nanoceramics

O.V. Palashov, E.A. Khazanov, I.B. Mukhin, A.N. Smirnov, I.A. Mironov, K.V. Dukel'skii, E.A. Garibin, P.P. Fedorov, S.V. Kuznetsov, V.V. Osiko, T.T. Basiev, R.V. Gainutdinov

***Abstract*. The optical characteristics of two Russian-made CaF_2 ceramic samples are compared to those of single-crystal CaF_2. The results indicate that the ceramic possesses high optical quality and a small absorption coefficient ($\sim 10^{-3}$ cm^{-1} at a wavelength of 1.07 μm) and is suitable as a material for optical components. Experimental evidence is presented for spatial modulation of the thermally induced depolarisation in the ceramic.**

Keywords: *optical ceramics, fluorite, thermally induced depolarisation.*

1. Introduction

In recent years, polycrystalline ceramics with a cubic crystal structure have been used increasingly in laser technology as active and magneto-active media and *Q*-switch materials [1–7]. This is due to their unique properties, different from those of single crystals and glass. Ceramics have three main advantages that make them suitable for use in high average and peak power lasers. First, they have a large aperture (up to 450 mm [8, 9]), like glasses, and high thermal conductivity, like single crystals. Second, ceramics can be produced from materials that have attractive spectroscopic and mechanical properties (e.g., Y_2O_3, YAG and YScAG) but are difficult to prepare in single-crystal form. Finally, ceramics possess a large thermal shock resistance parameter (several times that of single crystals [7, 10]). Therefore, ceramics have considerable potential for use in high-power lasers.

O.V. Palashov, E.A. Khazanov, I.B. Mukhin Institute of Applied Physics, Russian Academy of Sciences, ul. Ulyanova 46, 603950 Nizhnii Novgorod, Russia; e-mail: palashov@appl.sci-nnov.ru;
A.N. Smirnov, I.A. Mironov, K.V. Dukel'skii Research Institute of Optical Materials Technology, S.I. Vavilov State Optical Institute, ul. Babushkina 36/1, 192171 St. Petersburg, Russia; e-mail: mia@atlant.ru;
E.A. Garibin INCROM Ltd., ul. Babushkina 36/1, 192171 St. Petersburg, Russia; e-mail: incrom@pop3.rcom.ru;
P.P. Fedorov, S.V. Kuznetsov, V.V. Osiko, T.T. Basiev Laser Materials and Technologies Research Center, A.M. Prokhorov General Physics Institute, Russian Academy of Sciences, ul. Vavilova 38, 119991 Moscow, Russia; e-mail: ppf@lst.gpi.ru;
R.V. Gainutdinov A.V. Shubnikov Institute of Crystallography, Russian Academy of Sciences, Leninsky prosp. 59, 119333 Moscow, Russia

Received 20 November 2008; revision received 5 March 2009
Kvantovaya Elektronika **39** (10) 943–947 (2009)
Translated by O.M. Tsarev

Modern technology enables the fabrication of quality ceramic optical components with a large aperture and high concentration of laser ions. Most effort has been concentrated on oxide laser ceramics (e.g., Nd : YAG and Cr : YAG). Until recently, only Japanese-made ceramic media were reported in the literature [11]. Reports on analogous materials made in Russia [12, 13], China [14] and the United States [15] have emerged only in the past few years.

In this paper, we present measurements of the optical characteristics of CaF_2 ceramics produced by hot pressing [16–18] at the Research Institute of Optical Materials Technology, S.I. Vavilov State Optical Institute, and at the Laser Materials and Technology Research Center, A.M. Prokhorov General Physics Institute, Russian Academy of Sciences. One distinctive feature of fluoride ceramics is their high optical transmission at wavelengths of up to ~ 10 μm. Rare-earth-doped CaF_2 crystals are used as gain media [19–21]. A $CaF_2 : Dy^{2+}$ laser ceramic was first produced by Hatch et al. [22]. Lasing of $LiF : F_2^-$ and $Ca_{0.6}Sr_{0.4}F_2 : Yb^{3+}$ fluoride ceramics was studied by Basiev et al. [23–25].

The purpose of this work was to compare the optical performance of single-crystal fluorite and transparent ceramics of the same composition by measuring the thermally induced depolarisation of laser radiation.

2. Sample preparation and characterisation

In our experiments, three CaF_2 samples were used. Two samples were cut from an artificial optical ceramic plate 100 mm in diameter. One of them (sample 1), $9 \times 14 \times 45$ mm in dimensions, was cut from the central part of the plate and was used in previous studies [17, 26]. The other (sample 2), measuring $8 \times 12 \times 35$ mm (Fig. 1), was cut from the peripheral part of the plate. Sample 3, an [001]-oriented single crystal measuring $9 \times 12.5 \times 45$ mm, was cut from an ingot grown by vertical directional solidification.

The ceramic plate was produced by hot pressing in a vacuum of 5×10^{-3} Torr at 1100 °C and 200 MPa. The pressure was applied for 60 min.

The microstructure of the ceramic samples was examined using chemical etching and atomic force microscopy (AFM). The grain structure was revealed by etching an abrasively polished sample surface with sulphuric acid. AFM images were obtained in contact mode on a SOLVER P47H microscope (NT-MDT, Russia), using silicon cantilevers (TL02, MikroMasch, Estonia) with a resonance frequency of ~ 60 kHz and a force constant of ~ 3 N m^{-1}. All the

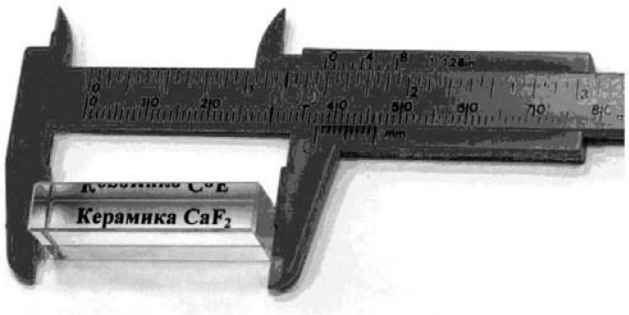

Figure 1. Visual appearance of sample 2.

measurements were made in air at room temperature under clean-room conditions (Trackpore Room 02). The temperature and humidity were maintained with a stability of $\pm 0.05\,\%$ and $\pm 1\,\%$, respectively.

The polycrystalline ceramics studied consists of single-crystal grains ~ 100 μm in size, separated by thin boundaries (Figs 2a, b [17, 27]). Each grain has a lamellar microstructure with a separation between the lamellae less than 100 nm (Fig. 2c), which seems to be due to twinning processes during the fabrication of the ceramic.

3. Absorption measurements

One important distinction of ceramics from single crystals is that the crystallographic axes in the grains of ceramics are randomly oriented. Because CaF_2 single crystals are optically isotropic, CaF_2 ceramics are also optically isotropic. Radiation absorption in ceramics leads to heat release and, hence, to temperature gradients, giving rise to mechanical stress. By virtue of the photoelastic effect, the mechanical stress leads to thermally induced depolarisation of the transmitted beam, which can be quantified by the degree of depolarisation, γ_T. The spatial distribution of γ_T is known to have the form of a Maltese cross (see, e.g., Ref. [28]). As distinct from the irregular structure of 'cold' depolarisation, in the case of a small heat release the γ_T of a Gaussian beam transmitted through an [001]-oriented cylindrical crystal [29] or ceramics [30, 31] is given by

$$\gamma_{T[001]} = 0.137\frac{p^2}{8}[1 + (\xi^2 - 1)\cos^2(2\theta)], \tag{1}$$

$$\gamma_{T\mathrm{cer}} = 0.137\frac{p^2}{8}\left(\frac{1 + 2\xi_{\mathrm{eff}}}{3}\right)^2,$$

where

$$p = \frac{Q\alpha LP_0}{\lambda k}; \quad Q = \alpha_T\frac{n_0^2}{4}\frac{1+v}{1-v}(p_{11} - p_{12});$$

$$\xi = \frac{2p_{44}}{p_{11} - p_{12}}; \quad \xi_{\mathrm{eff}} = 1 + (\xi - 1)\frac{225}{256}; \tag{2}$$

α is the absorption coefficient of the material; λ is the laser wavelength; θ is the angle between the polarisation direction and one of the crystallographic axes; L is the sample length; and P_0 is the transmitted power. The other constants are given below. Therefore, from an experimentally determined degree of thermally induced depolarisation, γ_T, and material's parameters, one can evaluate its absorption coefficient, α, using relations (1) and (2).

Photoelastic constants

p_{11}	0.056 [28], 0.035 [32, 33]
p_{12}	0.228 [28], 0.127 [32, 33]
p_{44}	−0.024 [28], 0.042 [32, 33]
Photoelastic anisotropy parameter ξ	0.3 [28], −0.9 [32, 33]
Thermal conductivity $k/\mathrm{W\,K^{-1}m^{-1}}$	10.3
Poisson's ratio v	0.24
Index of refraction n_0	1.428
Linear expansion coefficient $\alpha_T/\mathrm{K^{-1}}$	18×10^{-6}

4. Experimental results

Figure 3 shows a schematic of the setup used to measure the degree of thermal depolarisation. The 1.07-μm radiation from an ytterbium fibre laser (*1*) with an output power of up to 330 W was used both to heat the sample and to measure the polarisation. The beam had a Gaussian intensity distribution, and its diameter was controlled by varying the magnification factor of the telescope (*2*). The beam was linearly polarised by a spar wedge (*3*) placed in front of the sample (*4*). Another spar wedge (*5*) was oriented so as to minimise the beam intensity reaching the CCD camera (*7*). The spar wedges ensured a contrast of at least 10^5. In the presence of a sample, the radiation

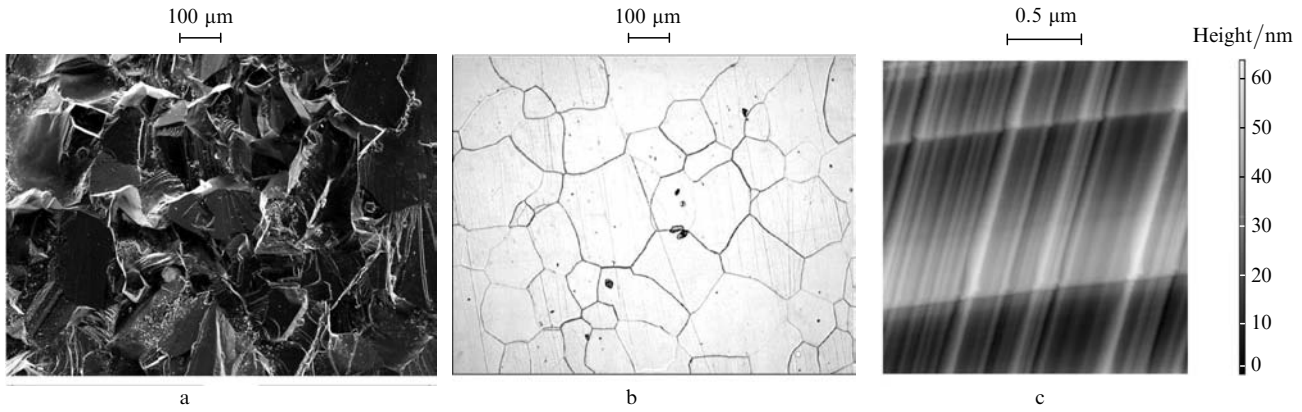

Figure 2. Micro- and nanostructure of the CaF_2 ceramic: (a) scanning electron micrograph of a fracture surface (JEOL JSM-5910); (b) polished and etched sample surface (LOMO μVizo-103 digital microscope), field dimensions of 1.07×0.80 mm; (c) AFM image of a fracture surface.

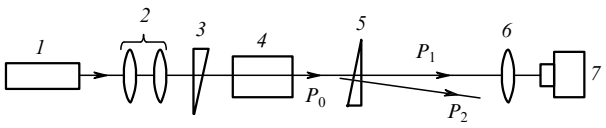

Figure 3. Schematic of the experimental setup: (*1*) laser; (*2*) telescope; (*3*, *5*) spar wedges; (*4*) sample; (*6*) lens; (*7*) CCD camera.

reaching the CCD camera was depolarised. The image of the exit face of the sample was relayed to the CCD camera (*7*) via a lens (*6*). The degree of depolarisation was determined as

$$\gamma = P_1/P_0. \tag{3}$$

Here, $P_0 = P_1 + P_2$, where P_1 and P_2 are the depolarised and polarised beam powers.

Figure 4 presents the results of cold-depolarisation measurements at a laser output power of 1 W, which characterise the quality of the three samples. The 1/e beam diameter was 12 mm. It can be seen, first, that the depolarisation in the single crystal is substantially smaller than that in the ceramic samples and, second, that the depolarisation in samples 1 (ceramic) and 3 (single crystal) is more nonuniform than that in sample 2 (ceramic) and is considerably greater in the corners of the aperture. This may be due to cutting- or processing-induced stresses.

Figure 5 shows the measured degree of depolarisation as a function of laser output power for the three samples. The laser beam diameter was 1.5 mm. The measurement areas are circled in Fig. 4. As seen in Fig. 5, the degree of cold depolarisation in the single crystal is within 10^{-4} and exceeds the degree of thermally induced depolarisation over the entire range of beam powers studied. For this reason, the absorption coefficient cannot be accurately evaluated. From the present measurement results and the photoelastic constants reported by Mezenov et al. [28] (the most reliable in our opinion), we infer that $\alpha < 2\times 10^{-4}$ cm^{-1}. At the same time, the degree of cold depolarisation in the ceramic samples (no greater than 10^{-3}) considerably exceeds that in the single crystal but is acceptable for most applications. At laser output powers above 100 W (Fig. 5), the degree of thermally induced depolarisation in the ceramic samples exceeds the degree of cold depolarisation and rises quadratically with beam power, in accordance with formulas (1) and (2). The absorption coefficient evaluated as described above is 1.09×10^{-3} and 1.5×10^{-3} cm^{-1} in the ceramic samples 1 and 2, respectively. Note that the absorption in areas other than those circled in Fig. 4 was stronger and that the depolarisa-

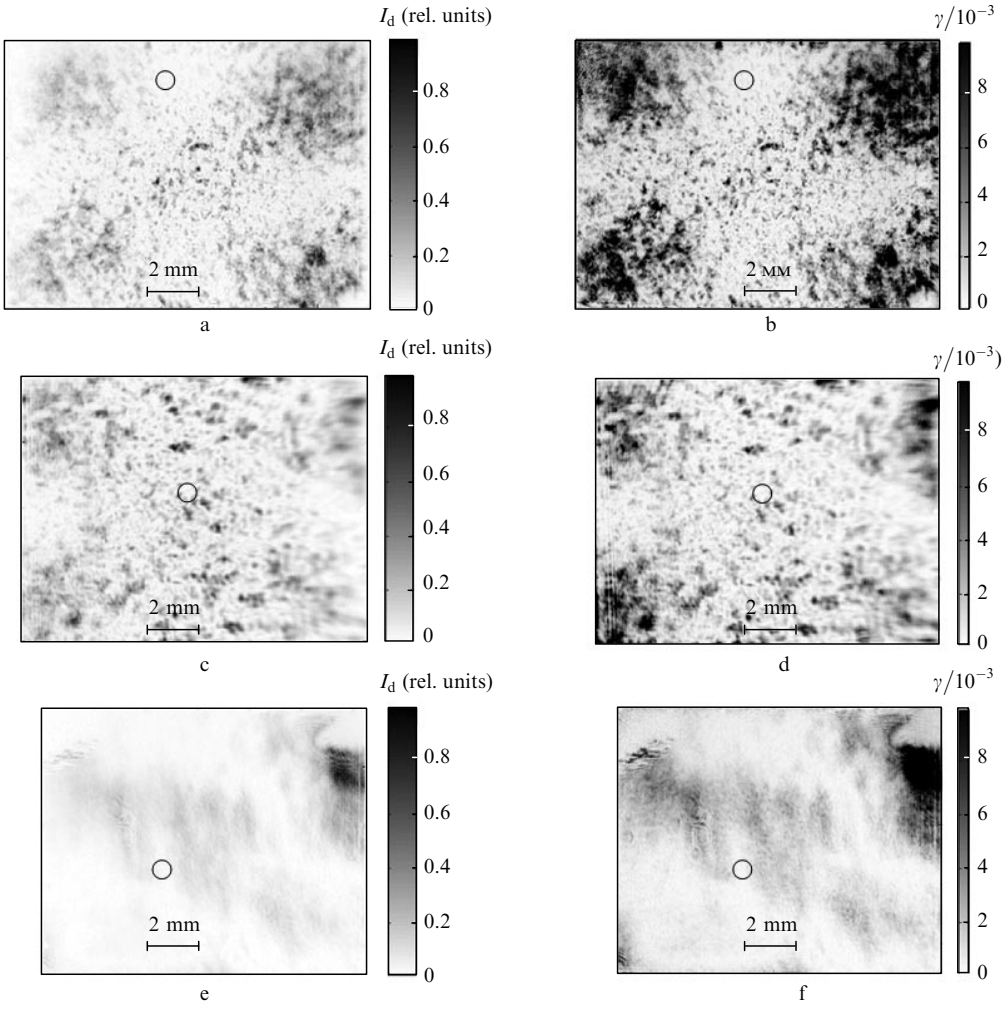

Figure 4. Spatial distributions of (a, c, e) the intensity of the depolarised beam, I_d, and (b, d, f) the degree of depolarisation, γ, for the ceramic samples (a, b) 1 and (c, d) 2 and (e, f) the single-crystal sample at a laser output power of 1 W.

tion in sample 1 was more nonuniform than that in sample 2. In Fig. 5, the triangles represent the measurement results obtained for two different areas on sample 1 at a beam diameter of 1.5 mm. Sample 2 was considerably more homogeneous than sample 1. The circles in Fig. 5 represent the measurement results obtained for nearly the same area of the sample at two different beam diameters. As seen, increasing the beam diameter from 1.5 to 4.2 mm increases the degree of depolarisation only slightly, by no more than a factor of 2.

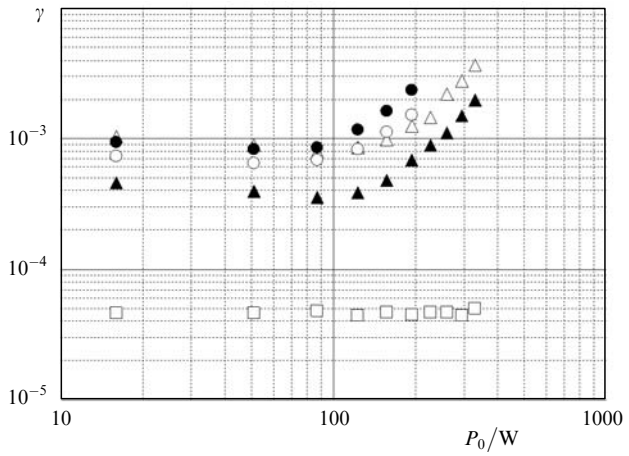

Figure 5. Degree of depolarisation as a function of laser output power for ceramic samples 1 (△, ▲) and 2 (○, ●) and the single-crystal sample (□) at beam diameters of 4.2 (●) and 1.5 mm (other data points).

At laser output powers above 200 W, the transverse intensity profile of the depolarised beam takes the shape of a Maltese cross (Fig. 6a). The transverse intensity modulation cannot be accounted for by the nonideality of the ceramic because, even when absorption varies from grain to grain, the length scale of temperature variations across the sample in the steady-state temperature distribution cannot be less than 1 mm. The transverse intensity modulation of the depolarised beam is due to the fact that the photoelastic effect depends on the orientation of the crystallographic axes in the grains [30, 31]. Because of the random orientation of the axes in the grains, the degree of depolarisation is a random function.

Figure 7 shows the experimentally determined and calculated rms deviations in the degree of depolarisation as functions of the laser output power. The experimental rms deviation was evaluated as the deviation from the calculated average intensity of the depolarised beam [30]. The theoretical value of the rms deviation was computed using a procedure described elsewhere [31]. It involves numerical modelling of a large number of ceramic samples composed of randomly oriented, randomly arranged single-crystal grains and computation of the polarisation distortion in a laser beam passing through the grains. The ensemble is then used to compute the rms deviation. Figure 7 presents the rms deviations obtained for two combinations of photoelastic constants. Note that both the experimentally determined and theoretical values of the rms deviation are comparable to the degree of depolarisation and increase with transmitted power. The contribution to the rms deviation from the nonuniformity of the cold depolarisation and intensity in the beam transmitted through the ceramic is

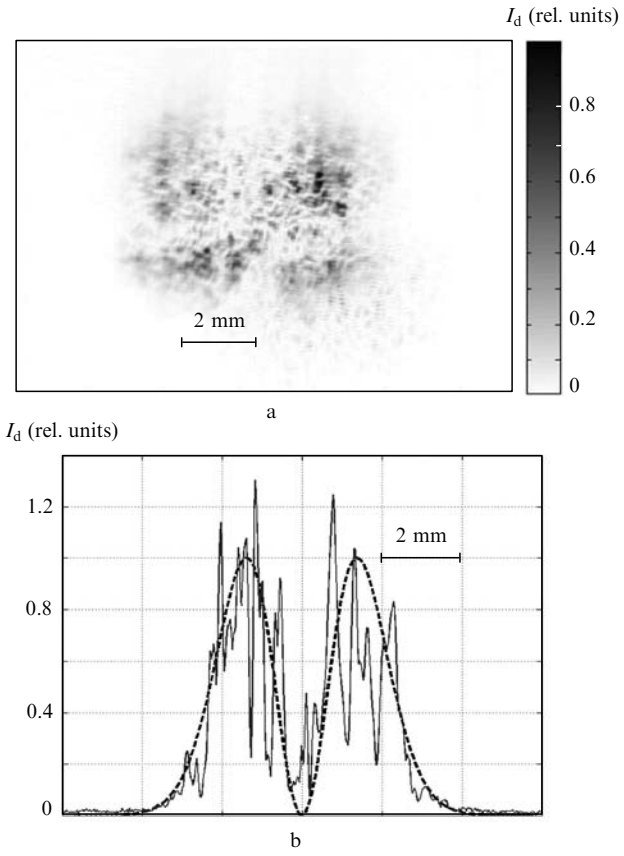

Figure 6. (a) Transverse distribution of the depolarised beam intensity, I_d, for sample 2 at a laser output power of 200 W and (b) a section through the distribution. The dashed line represents the corresponding theoretical values.

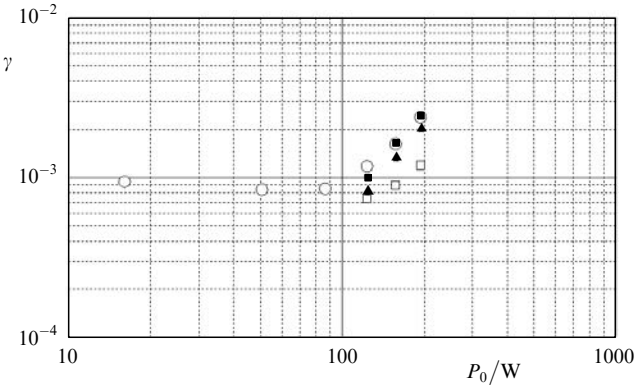

Figure 7. Degree of depolarisation (○) and experimentally determined (□) and theoretical values of its rms deviation as functions of the laser output power for ceramic sample 2; average grain size, 100 μm; $\xi = 0.3$ (■) and $\xi = -0.9$ (▲).

within 8×10^{-4}. The experimentally determined and theoretical values of the rms deviation do not coincide, but the increase in both values with the output laser power points to dispersion of thermally induced depolarisation in the ceramic, the effect that was described previously [30, 31].

5. Conclusions

Comparison of the optical characteristics of a CaF_2 single crystal and two CaF_2 laser ceramic samples demonstrates

that the ceramic, even though inferior in optical performance to the single crystal, offers high optical quality and a small absorption coefficient ($\sim 10^{-3}$ cm^{-1}) at a wavelength of 1.07 μm and is suitable as a material for optical components. The optical losses in the ceramic samples seem to be due to grain-boundary scattering.

Our experimental data provide evidence for spatial modulation of the thermally induced depolarisation in the ceramic.

Acknowledgements. This work was supported in part by the Russian Foundation for Basic Research (Grant No. 08-03-12080ofi) and the Federal Agency for Science and Innovations (State Contract No. 02.513.12.3029). S.V. Kuznetsov acknowledges the support from the Regional Public Foundation for National Science Promotion.

References

1. Ikesue A., Kinoshita T., Kmata K., Yoshida K. *J. Am. Ceram. Soc*., **78**, 1033 (1995).
2. Khazanov E.A. *Opt. Lett*., **27** (9), 716 (2002).
3. Lu J.R., Lu J.H., Murai T., Takaichi K., Uematsu T., Ueda K., Yagi H., Yanagitani T., Kaminskii A.A. *Jap. J. Appl. Phys. Part 2–Lett*., **40** (12A), L1277 (2001).
4. Takaichi K., Lu J.R., Murai T., Uematsu T., Shirakawa A., Ueda K., Yagi H., Yanagitani T., Kaminskii A.A. *Jpn. J. Appl. Phys., Part 2*, **41** (2A), L96 (2002).
5. Kagan M.A., Khazanov E.A. *Appl. Opt*., **43** (32), 6030 (2004).
6. Kaminskii A.A., Eichler H.J., Ueda K., Bagaev S.N., Gad G.M.A., Lu J., Murai T., Yagi H., Yanagitani T. *Phys. Status Solidi A*, **181** (2), R19 (2000).
7. Kaminskii A.A., Akchurin M.Sh., Alshits V.I., Ueda K., Takaichi K., Lu J., Uematsu T., Musha M., Shirakawa A., Gabler F., Eichler H.J., Yagi H., Yanagitani T., Bagayev S.N., Fernandez J., Balda R. *Kristallografiya*, **48** (3), 562 (2003).
8. Lu J., Prabhu M., Xu J., Ueda K., Yagi H., Yanagitani T., Kaminskii A.A. *Appl. Phys. Lett*., **77** (23), 3707 (2000).
9. Lu J., Song J., Prabhu M., Xu J., Ueda K., Yagi H., Yanagitani T., Kudryashov A. *Jpn. J. Appl. Phys., Part 2*, **39** (10B), L1048 (2000).
10. Ueda K. *Intern. Conf. on Lasers, Applications, and Technologies* (St. Petersburg, 2005) p. LWG2.
11. Yanagitani T., Yagi H., Yamasaki Y. Japan Patent, 10-101411, 1998.
12. Bagaev S.N., Osipov V.V., Ivanov V.I., Solomonov V.I., Platonov V.V., Orlov A.N., Rasuleva A.V., Ivanov V.V., Kaigorodov A.S., Khrustov V.R., Vatnik S.M., Vedin I.A., Maiorov A.P., Pestryakov E.V., Shestakov A.V., Salkov A.V. *Kvantovaya Elektron*., **38** (9), 840 (2008) [*Quantum Electron*., **38** (9), 840 (2008)].
13. Kaminskii A.A., Kravchenko V.B., Kopylov Yu.L., Bagayev S.N., Shemet V.V., Komarov A.A., Kallmeyer F., Eichler H.J. *Phys. Status Solidi A,* **204** (7), 2411 (2007).
14. Wu Yusong, Li Jiang, Pan Yubai, Guo Jingkun, Liu Qian. *Adv. Mater. Res*., **15-17**, 246 (2007); online at http://www.scientific.net.
15. Ostby E.P., Ackerman R.A., Huie J.C., Gentilman R.L. *Proc. SPIE–Int. Soc. Opt. Eng*., **6100**, 610004 (2006).
16. Volynets F.K. *Izv. Akad. Nauk SSSR, Ser. Fiz*., **45** (2), 315 (1981).
17. Popov V.A., Dukel'skii K.V., Mironov I.A., Smirnov A.N., Smolyanskii P.A., Fedorov P.P., Osiko V.V., Basiev T.T. *Dokl. Akad. Nauk*, **412** (2), 185 (2007).
18. Fedorov P.P., Osiko V.V., Basiev T.T., Orlovskii Yu.V., Dukel'skii K.V., Mironov I.A., Demidenko V.A., Smirnov A.N. *Ross. Nanotekhnol*., **2** (5-6), 95 (2007).
19. Liangbi Su, Jun Xu, Yinghong Xue, Chingyue Wang, Lu Chai, Xiaodong Xu, Guangjun Zhao. *Opt. Express*, **13** (15), 5635 (2005).
20. Basiev T.T., Orlovskii Yu.V., Polyachenkova M.V., Fedorov P.P., Kuznetsov S.V., Konyushkin V.A., Osiko V.V., Alimov O.K., Dergachev A.Yu. *Kvantovaya Elektron*., **36** (7), 591 (2006) [*Quantum Electron*., **36** (7), 591 (2006)].
21. Basiev T.T., Vasil'ev S.V., Doroshenko M.E., Konyushkin V.A., Kuznetsov S.V., Osiko V.V., Fedorov P.P. *Kvantovaya Elektron*., **37** (10), 934 (2007) [*Quantum Electron*., **37** (10), 934 (2007)].
22. Hatch S.E., Parson W.F., Weagley R.J. *Appl. Phys. Lett*., **5** (8), 153 (1964).
23. Basiev T.T., Doroshenko M.E., Konyushkin V.A., Osiko V.V., Ivanov L.I., Simakov S.V. *Kvantovaya Elektron*., **37** (11), 989 (2007) [*Quantum Electron*., **37** (11), 989 (2007)].
24. Basiev T.T., Doroshenko M.E., Fedorov P.P., Konyushkin V.A., Kouznetsov S.V., Voronov V.V., Osiko V.V. *Adv. Sol. State Photonics Conf. Program and Techn. Dig*. (Nara, Japan, 2008) MC14.
25. Basiev T.T., Doroshenko M.E., Fedorov P.P., Konyushkin V.A., Kuznetsov S.V., Osiko V.V., Akchurin M.Sh. *Opt. Lett*., **33** (5), 521 (2008).
26. Palashov O.V., Khazanov E.A., Mukhin I.B., Mironov I.A., Smirnov A.N., Dukel'skii K.V., Fedorov P.P., Osiko V.V., Basiev T.T. *Kvantovaya Elektron*., **37** (1), 27 (2007) [*Quantum Electron*., **37** (1), 27 (2007)].
27. Khazanov E.N., Taranov A.V., Fedorov P.P., Kuznetsov S.V., Basiev T.T., Mironov I.A., Smirnov A.N., Dukel'skii K.V., Garibin E.A. *Dokl. Akad. Nauk*, **424** (3), 326 (2009).
28. Mezenov A.V., Soms L.N., Stepanov A.I. *Termodinamika tverdotel'nykh lazerov* (Thermodynamics of Solid-State Lasers) (Leningrad: Mashinostroenie, 1986).
29. Mukhin I.B., Palashov O.V., Khazanov E.A., Ivanov I.A. *Pis'ma Zh. Eksp. Teor. Fiz*., **81**, 120 (2005).
30. Kagan M.A., Khazanov E.A. *Kvantovaya Elektron*., **33**, 876 (2003) [*Quantum Electron*., **33**, 876 (2003)].
31. Mukhin I., Palashov O., Khazanov E., Ikesue A., Aung Y. *Opt. Express*, **13** (16), (2005).
32. http://www.corning.com/docs/specialtymaterials/pisheets/H0607_CaF2_Product_Sheet.pdf.
33. http://www.schott.com/lithotec/english/download/lit-2_stress_optical_coefficients_fs_caf2_burnett.pdf.